STM Investigation of Nano-structures Fabricated on Passivated Si Surfaces

Jeong Sook Ha[†], Kang-Ho Park*, Kyoung-Wan Park* and Wan Soo Yun**

Department of Chemical and Biological Engineering, Korea University, Seoul 136-701, Korea
*Semiconductor Basic Research Laboratories, ETRI, Daejeon 305-600, Korea
**Electronic Devices Group, KRISS, Daejeon 305-600, Korea

Abstract−We have successfully fabricated nano-structures on passivated Si surfaces and investigated those structures by using scanning tunneling microscope (STM) and atomic force microscope (AFM). Ag nano-dots were formed on Sb-passivated Si(100) surface via self-organization mechanism and the single-electron charging effect was observed by STM at room temperature. Thermal nitridation and subsequent oxygen-induced etching of Si surfaces resulted in the formation of silicon nano-dots using silicon nitride islands as masks. Au/Ti nano-wire was also fabricated via a selective ion etching of Au/Ti thin film using carbon nanotube (CNT) mask. These results suggest new fabrication method of nano-structures using surface chemical reactions without artificial lithography techniques.

Key words: Nano-fabrication, Passivated Si Surfaces, Scanning Tunneling Microscope, Atomic Force Microscope, Ag Nano-dot, Si Nano-dot, Carbon Nanotube, Au Nano-wire

INTRODUCTION

Recently, there has been much effort to fabricate nano-structures such as dots and wires since they are expected to show many distinctive differences in electrical and optical properties from the bulk materials due to quantum confinement effect [Fisher and Chou, 1993; Chen and Ahmed, 1993; Goglides et al., 1995; Nassipoulos et al., 1995; Tada et al., 1998; Seeger and Palmer, 1999; Averin et al., 1991; Markovch et al., 1997; Chen et al., 1995; Tiwari et al., 1996; Rabe and Buchholz, 1991].

Up to now, two different approaches have been used: synthesis of nano-structures from atom and molecules vs. reduction of size from bulk materials via lithography or etching reaction. We found that deliberate control of surface chemical reactions can be used in the fabrication of nano-structures. We present three different kinds of fabrication method of (1) Ag nano-dots on Sb-passivated Si(100) surface (2) Si nano-dots on Si(100), Si(111), and SOI (silicon on insulator) substrates (3) Au/Ti nano-wires on SiO_2 surface. These are all based on the understanding of surface reactions, especially surface passivation, and our main objective is not to use artificial lithography techniques in the nano-fabrication.

In the first part, we discuss the growth of Ag nano-dots on Sb-paasivated Si(100) surface via self-organization mechanism and the observation of single electron tunneling phenomena at room temperature. In the second part, we will present the results on the formation of Si nano-dots on Si(100), Si(111), and SOI surfaces via thermal nitridation and subsequent oxygen induced etching reactions using silicon nitride islands as passivating masks. Finally, we will introduce the fabrication of Au/Ti nano-wire via selective Ar^+ etching using carbon nanotube as a mask.

EXPERIMENTAL

[†]To whom correspondence should be addressed.
E-mail: jeongsha@korea.ac.kr

1. Ag Nano-dots on Sb-terminated Si(100) Surface

Clean p-type Si(100) with a resistivity of 1 Ωcm was obtained via repeated flashing at 1,200 °C. Sb was deposited on the clean Si(100) surface at 375 °C. The absolute coverage of Sb was controlled at ca 1-2 monolayers (ML), and then the sample was annealed for several minutes at 550 °C in order to form a well-ordered Sb-terminated Si(100) surface. This post-annealing temperature lies well above the Sb_4 desorption temperature, leading to complete removal of unreacted Sb. As a result, not only the dangling bonds of Si are fully passivated by a dimerized Sb adlayer, but also the outermost Si layer showed bulk-like properties via the structural change from a (2×1) dimer reconstruction to bulk-like (1×1).

Ag was deposited on the Sb-terminated Si(100) under the deposition rate of 0.1-0.2 ML/min at room temperature. Ag was thermally evaporated from a hot tungsten filament at $3×10^{-10}$ Torr, and the coverage was monitored with a Quartz crystal oscillator. The STM images were obtained with a sample bias voltage of 3.0 V and tunneling current of 0.5 nA using a home-made STM system.

2. Si Nano-dots on Si(100), Si(111) and SOI Surfaces

A Si(100) surface of p type, 1 Ωcm was cleaned by repeated flashing at 1,200 °C. A Si(111) surface was flashed at 1,150 °C and then slowly cooled down to room temperature to produce a clean and well ordered Si(111)-7×7 surface with single atomic height steps. SOI sample was composed of 30 nm Si thin film/100 nm silicon oxide/Si(100) substrate. SOI substrate was BOE treated before installing inside the vacuum chamber and then it was flashed at 750 °C several times.

High purity nitrogen gas (99.999%) was dosed to the Si(100), Si(111), and SOI surfaces at 700 °C under a nitrogen partial pressure of $1×10^{-5}$ Torr. On these surfaces oxygen gas (99.999%) was exposed at temperatures between 700 and 800 °C under an oxygen partial pressure of $1×10^{-7}$ Torr, which is suitable for the selective etching of bare Si surfaces. All the STM measurements on Si(100) and Si(111) surfaces were performed at room temperature in a constant current mode. AFM measurement on SOI substrate was done

in air in a non-contact mode.

3. Au/Ti Nano-wire on SiO₂ Surface

A very thin Ti layer was deposited onto SiO₂ substrate, prior to the deposition of Au, to enhance the adhesion between the SiO₂ film and Au layer and to reduce the roughness of the Au surface. Ti and Au were successively deposited by e-beam evaporation under the operation pressure of less than 10^{-6} Torr on an oxide film (200 nm in thickness) thermally grown on a Si(111) wafer. The thickness of the Ti and Au layers was 1-2 and 9 nm, respectively, which was estimated by AFM after the formation of metal patterns by photolithography.

A few drops of a CNT suspension in CHCl₃ were spin coated on the Au/Ti/SiO₂/Si(111) surface at a spinning rate of 2,000 rpm. The CNTs were uniformly distributed on the whole surface, some of them entangled or bundled. The CNTs used in this work were multi-walled carbon nanotubes with typical diameters of 10-20 nm. To induce physical etching of the Au/Ti layer, Ar⁺ ions of 300 eV kinetic energy were bombarded at the normal incidence angle under the Ar partial pressure of 2.6×10^{-4} Torr (Ar⁺ ion milling). The nominal current of Ar⁺ ion beam and the irradiation time were set to be 10 mA and 1 min, respectively. Owing to the great difference in the milling rates between the CNTs and the metal layer, Au/Ti nano-
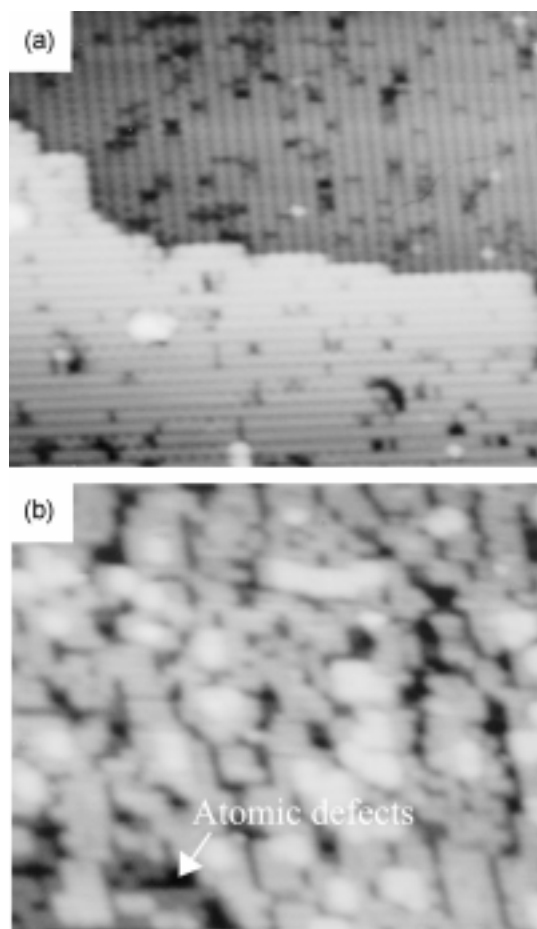

Fig. 1. STM images taken from (a) a clean Si(100) surface and (b) Sb-terminated Si(100) surface (scan area=22.5×22.5 nm²). Sb dimer rows are imaged bright and atomic defects such as missing Sb dimers are imaged dark.

wires were formed right underneath the CNTs and their bundles. By using the contact-mode AFM, the resultant structure of the Au/Ti nano-wires capped with the CNTs was carefully investigated.

RESULTS AND DISCUSSION

1. Ag Nano-dots on Sb-terminated Si(100) Surface

Fig. 1(a) and 1(b) show the STM images of a clean Si(100) surface and the Sb-terminated Si(100) surface, respectively. Due to a large 16% lattice mismatch between Sb and Si [Rich et al., 1989] and the corresponding compressed strain in dimer rows, the length of Sb dimer row cannot exceed a certain coherence length. Many atomic defects such as missing Sb dimers are formed and the average dimer length is estimated to be 2.5-2.6 nm. Tunneling current (I) vs. sample bias voltage (V) measurement showed that the surface gap states are absent in the Si band gap, indicating the passivation of Si dangling bonds by the Sb overlayer.

When Ag was deposited on this Sb-terminated Si(100) surface, small round clusters form already at submonolayer coverages, implying the absence of Ag wetting layer. At a nominal Ag coverage of 0.04 nm, the sizes of Ag dots are strikingly small (2-4 nm in diameter and 0.4-0.8 nm in height) and these were separated far from each other. The Ag dots reside on areas between the rows of Sb voids. I/V measurement showed that the forbidden gap (~1 eV) still existed on Ag dots of 0.04 nm film.

At the coverage of 0.2 nm, the sizes of Ag dots become 3-6 nm in diameter and 0.5-1.4 nm in height as shown in Fig. 2(a). Ag dots grown on Sb-terminated Si(100) surface are much smaller than those grown on Sb-terminated Si(111) at similar Ag coverages and have a quite narrow size distribution. This is explained in terms of the separation mechanism of Ag condensation by the underlying atomic defects, that is the aligned voids of Sb dimers [Park et al., 1998].

Most of the densely populated Ag dots shown in Fig. 2(a) revealed metallic conduction behavior. However, there were also a few Ag dots such as 'g', which is adjacent to another dot 'h' connected to densely populated Ag dot regions. The Ag dot 'g' showed reproducible I-V curves of single electron tunneling at room temperature. Coulomb blockade and staircases were clearly observed as shown in Fig. 2(b). Those are explained in terms of single electron tunneling via lateral tunneling between adjacent Ag dots [Park et al., 2000].

2. Si Nano-dots on Si(100) and Si(111) Surfaces

At high temperatures, two competing oxidation reactions, i.e., etching and oxide formation, occur on Si surfaces depending upon the partial pressure of oxygen gas. At higher oxygen gas pressure, oxide formation dominates the etching and surface etching dominates at lower oxygen pressure. On the other hand, our previous study showed that nitrogen exposure to Si surfaces at temperatures between 700-800 °C induces the growth of silicon nitride nano-islands [Ha et al., 1999]. From these two simple reactions, we can design the fabrication recipe of silicon nano-dots on Si surfaces as shown in Fig. 3. In the first step, we exposed N₂ gas to Si(100) and Si(111) surfaces at 700-800 °C under N₂ pressure of 1×10^{-5} Torr to form nano-sized silicon nitride islands. After that, oxygen gas was dosed to this silicon nitride covered Si surfaces under the condition of selective etching of Si surfaces with an oxygen partial pressure of 1×10^{-7} Torr. Then Si nano-dots capped with silicon nitride islands are
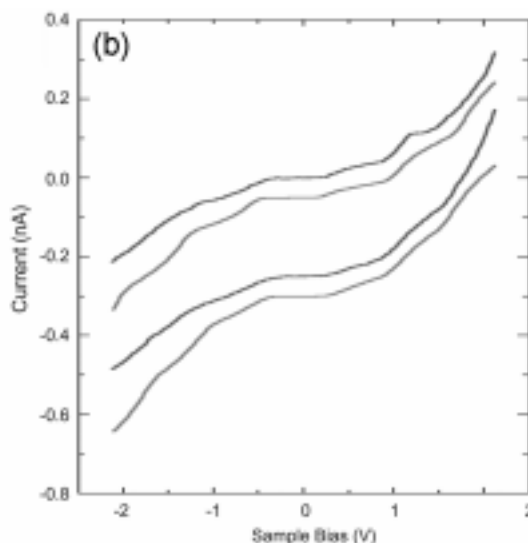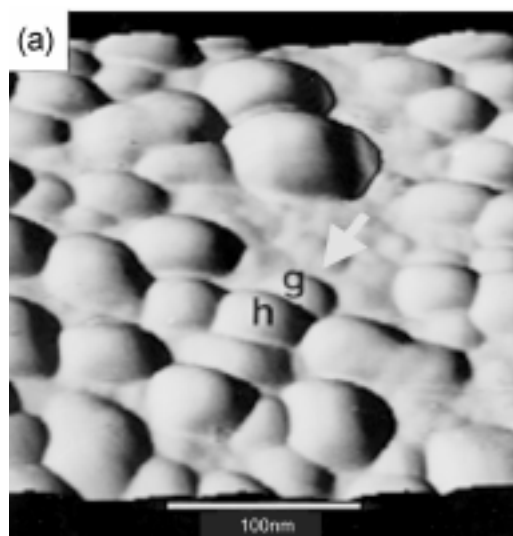
Fig. 2. (a) STM image taken from Ag dots grown on Sb-terminated Si(100) surface at a Ag coverage of 0.2 nm. (b) Tunneling I-V measurements on Ag dot 'g' with variation of tip-sample distance. The upper set of curves has smaller tip-dot distance by ~0.1 nm. For each set, lower curve is the least squares fitted one.
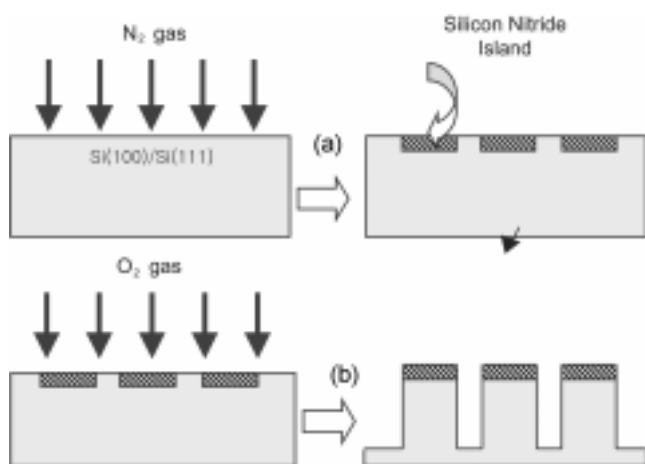

Fig. 3. Schematics of formation of silicon nano-dots on Si surfaces via (a) thermal nitridation and (b) oxygen induced etching reactions.

expected to be formed via selective etching of Si areas.

Fig. 4 shows the STM images of the Si(100) and Si(111) surfaces after the nitridation and subsequent oxygen induced etching reaction. As clearly seen in the images, on both surfaces, silicon nano-dots were formed. On Si(100) surface, Si nano-dots with a very uniform sizes were formed whereas, quite broad size distribution of nano-dots were observed on Si(111) surface. The average sizes were estimated to be 5 nm and 12.5 nm, respectively under the same reaction conditions. This can be explained in terms of different thermal mobility and symmetry between silicon nitride and substrate Si [Ha et al., 2001]. The lower thermal mobility of the nitrogen species on the Si(100) surface than on the Si(111) surface resulted in the formation of silicon nano-dots with much smaller sizes and higher number density. The improper match in the surface lattice constants and in the symmetry between silicon nitride and the Si(100) surface restricted the size of the silicon dots to a

few nanometers.

Fig. 5(a) and 5(b) show the AFM image and the schematic drawing for the resultant structure taken from the SOI sample after thermal nitridation and subsequent oxygen induced etching reactions. Silicon pillars with a height of ~30 nm were formed by complete etching of top silicon thin layer (~30 nm) of SOI sample. These pillars are considered to be electrically isolated and to be used in the electronic devices.

4. Au/Ti Nano-wire using CNT Mask

We have fabricated the metal nano-wires on an insulating substrate using carbon nanotubes as a new kind of mask material. Under the Ar^+ ion bombardment, it was reported that the etch rate of Au is much greater than that of CNTs [Behrich, 1981]. By irradiating Ar^+ ions of 300 eV energy on a nanotube coated Au/Ti thin layer on a SiO_2 substrate, Au/Ti nano-wires were successfully formed just underneath the nanotube, indicating that carbon nanotube has acted as a good mask against the argon ion bombardment.

Fig. 6(a) shows the experimental scheme and 6(b) shows the AFM images of the resultant Au/Ti nano-wire. Owing to the great difference in the etch rate between Au/Ti and CNTs, it is expected that only the bare Au/Ti thin film should be etched away while the area covered by CNTs not be etched away. As shown in the AFM image, Au/Ti nano-wires capped with CNTs were formed. The average height, width, and length of the structure obtained with excluding both end portions of the structure were 18 nm, 55 nm, and 1.6 μm, respectively.

To obtain an AFM image of the CNTs/metal nano-structure without possible tip crashing to the protruding surface structure, the experimental parameters of AFM measurement were carefully set and maintained; force exerted on the AFM tip, the sensitivity of feedback loop, and the scan speed were respectively set extremely small (~pN), sufficiently high (but not too high), and very low. During the scan of a large area, some of the CNTs might be removed from CNT bundle/metal structure because of relatively fast scan speed. As for the width of the structure, it can be affected by the finite tip
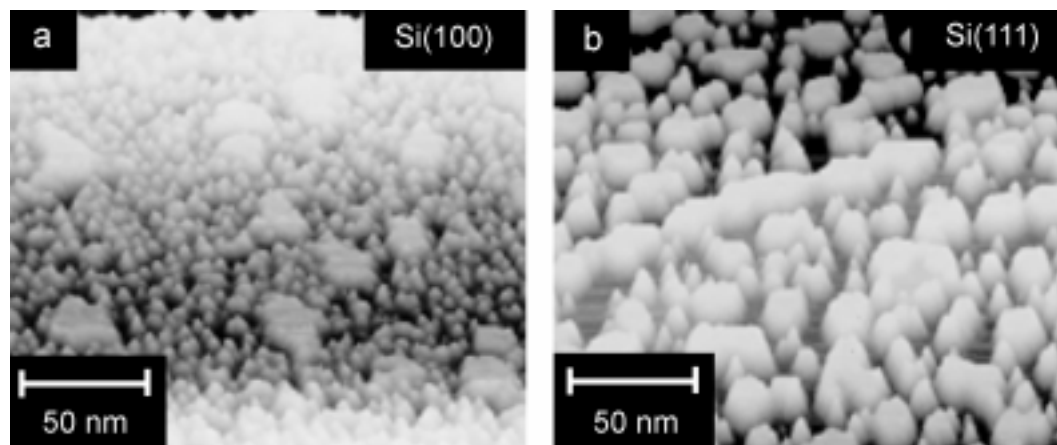
Fig. 4. STM images taken from Si(100) and Si(111) surfaces after thermal nitridation and oxygen induced etching reactions.
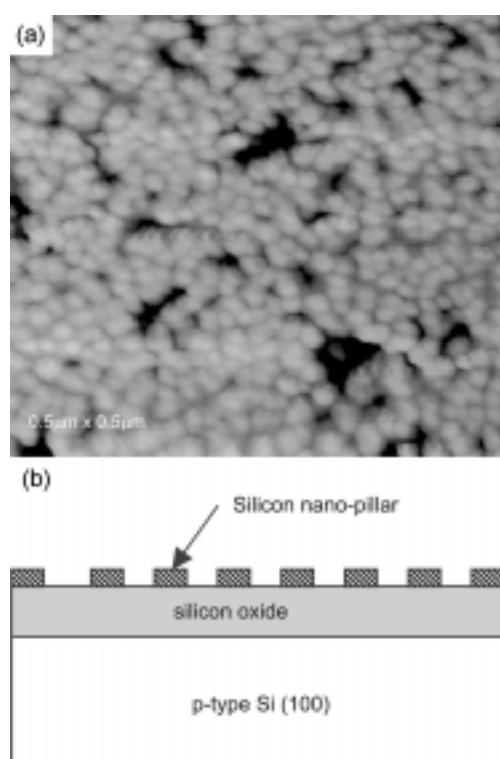

Fig. 5. (a) AFM image taken from SOI substrate after thermal nitridation and oxygen induced etching reactions and (b) the resultant structure on SOI sample.

size. When the set force on the AFM tip was increased to ~1nN, CNTs on the metal nano-wire were readily removed from the nano-wire structure as shown in Fig. 6(b). The average height and width of the Au/Ti nano-wire became 11 and 32 nm, respectively. The width of 32 nm is much smaller than that of the nano-wire capped with CNT before the removal of CNT. This can be explained in terms of the effect of finite tip size, which becomes less pronounced when the height of the protrusion is decreased. However, we cannot rule out the possibility that the CNT-covered nano-wire is actually wider than the Au/Ti metal nano-wire. The Au/Ti wire of a few nanometers in width was also frequently observed among the wires of various widths of a few tens of nm.
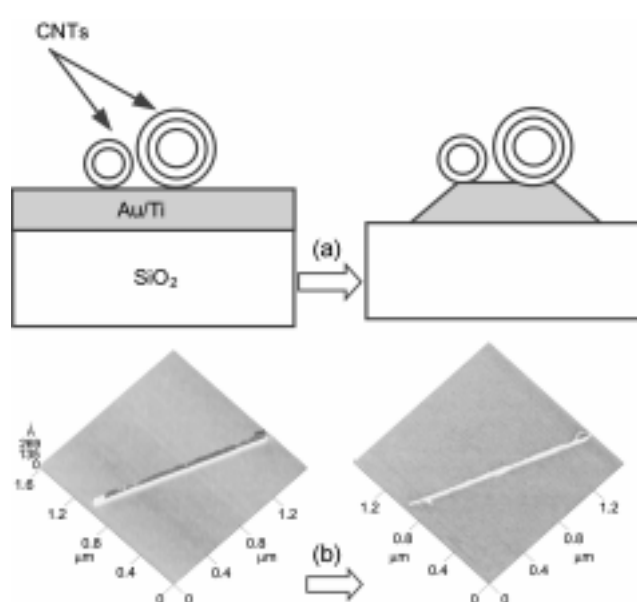
Fig. 6. (a) Schematics of the fabrication of Au/Ti nano-wire via selective Ar$^+$ ion bombardment of Au/Ti using CNT mask. (b) AFM images of Au/Ti nano-wire capped with CNT and without CNT.

CONCLUSIONS

We have devised three different fabrication method of nano-structures: Ag nano-dots on Sb-terminated Si(100) surface, Si nano-dots on Si(100), Si(111), and SOI surfaces and Au/Ti nano-wire on SiO$_2$ surface. All these nano-fabrication method are based on the deliberate control of surface chemical reactions without use of artificial lithography technique. These can be applied to the fabrication of nano-devices such as single electron transistor.

ACKNOWLEDGMENTS

REFERENCES

Averin, D. V. and Likharev, K. K. in: Altshuler, B. L., Lee, P. A. and Webb, R. A. (Eds.), "Mesoscopic Phenomena in Solids," Chap. 6, North-Holland, New York (1991).

Behrish, R., "Sputtering by Particle Bombardment," Springer, Berlin (1981).

Chen, W. and Ahmed, H., "Fabrication of High Aspect Ratio Silicon Pillars of <10 nm Diameter," *Appl. Phys. Lett.*, **63**, 1116 (1993).

Chen, W., Ahmed, H. and Nakazoto, K., "Coulomb Blockade at 77 K in Nanoscale Metallic Islands in a Lateral Nanostructure," *Appl. Phys. Lett.*, **66**, 3383 (1995).

Fischer, B. and Chou, S. Y., "Sub-50 nm High Aspect Ratio Silicon Pillars, Ridges, and Trenches Fabricated using Ultrahigh Resolution Electron Beam Lithography and Reactive Ion Etching," *Appl. Phys. Lett.*, **62**, 1414 (1993).

Goglides, E., Grigoropoulos, S. and Nassiopoulos, A. G., "High Anisotropic Room-temperature Sub-half-micron Si Reactive Ion Etching using Fluorine Only Containing Gases," *Microelectron. Eng.*, **27**, 449 (1995).

Ha, J. S., Park, K.-H., Ko, Y.-J., Yun, W. S. and Kim, S.-K., "Interaction of Nitrogen with Si(111)-7×7 Surfaces at Elevated Temperatures," *Surf. Sci.*, **426**, 373 (1999).

Ha, J. S., Park, K.-H., Yun, W. S. and Ko, Y.-J., "Thermal Nitridation and Oxygen-induced Etching Reactions: A Comparative Study on Si(100) and (111) Surfaces by Scanning Tunneling Microscope," *Jpn. J. Appl. Phys.*, **40**, 2429 (2001).

Markovich, G., Leff, D. V., Chung, S.-W., Soyez, H. M., Dun, B. and Heath, J. R., "Parallel Fabrication and Single-electron Charging of Devices Based on Ordered, Two-dimensional Phases of Organically Functionalized Metal Nanocrystals," *Appl. Phys. Lett.*, **70**, 3107 (1997).

Nassipoulos, G., Grigoropoulos, S., Goglides, E. and Papadimitrou, D., "Visible Luminescence from One- and Two-dimensional Silicon Structures Produced by Conventional Lithographic and Reactive Ion Etching Techniques," *Appl. Phys. Lett.*, **66**, 1114 (1995).

Park, K.-H., Ha, J. S., Yun, W. S. and Lee, E.-H., "Self-organization of Uniform Ag Nano-clusters on Sb-terminated Si(100) Surface," *Surf. Sci.*, **415**, 320 (1998).

Park, K.-H., Ha, J. S., Yun, W. S., Shin, M. and Ko, Y.-J., "Coulomb Staircases by Lateral Tunneling Between Adjacent Nanoclusters Formed on Si Surfaces," *J. Vac. Sci. Technol. A*, **18**, 2365 (2000).

Rabe, J. P. and Buchholz, S., "Fast Nanoscale Modification of Ag(111) using a Scanning Tunneling Microscope," *Appl. Phys. Lett.*, **68**, 1377 (1996).

Rich, D. H., Franklin, G. E., Leibsle, F. M., Miller, T. and Chiang, T. C., "Synchrotron Photoemission Studies of the Sb-passivated Si Surfaces: Degenerate Doping and Bulk Band Dispersions," *Phys. Rev. B*, **40**, 11804 (1989).

Seeger, K. and Palmer, R. E., "Fabrication of Silicon Cones and Pillars using Rough Metal Films as Plasma Etching Masks," *Appl. Phys. Lett.*, **74**, 1627 (1999).

Tada, T., Kanayama, T., Koga, K., Seeger, K., Carroll, S. J., Weibel, P. and Plmer, R. E., "Fabrication of Size-controlled 10 nm Scale Si Pillars using Metal Clusters as Formation Nuclei," *Microelectron. Eng.*, **41/42**, 539 (1998).

Tada, T., Kanayama, T., Koga, K., Weibel, P., Carroll, S. J., Seeger, K. and Plmer, R. E., "Formation of 10 nm Si Structures using Size-selected Metal Clusters," *J. Phys. D*, **31**, L21 (1998).

Tiwari, S., Rana, F., Hanafi, H., Hartstein, A., Crabb, E. F. and Chan, K., "A Silicon Nanocrystals Based Memory," *Appl. Phys. Lett.*, **68**, 1377 (1996).